HHS Public Access

Author manuscript

Behav Brain Res. Author manuscript; available in PMC 2021 March 02.

Published in final edited form as:

Behav Brain Res. 2020 March 02; 381: 112451. doi:10.1016/j.bbr.2019.112451.

Improved survival and overt "dystonic" symptoms in a torsinA hypofunction mouse model

Fumiaki Yokoi[a], **Fangfang Jiang**[a,b], **Kelly Dexter**[a], **Bryan Salvato**[a], **Yuqing Li**[a,1]

[a]Department of Neurology and Norman Fixel Institute of Neurological Diseases, College of Medicine, University of Florida, Gainesville, Florida, USA

[b]Wuxi Medical School, Jiangnan University, Wuxi, Jiangsu, PR China

Abstract

DYT1 dystonia is an inherited movement disorder without obvious neurodegeneration. Multiple mutant mouse models exhibit motor deficits without overt "dystonic" symptoms and neurodegeneration. However, some mouse models do. Among the later models, the N-CKO mouse model, which has a heterozygous *Tor1a*/*Dyt1* knockout (KO) in one allele and *Nestin-cre*-mediated conditional KO in the other, exhibits a severe lack of weight gain, neurodegeneration, overt "dystonic" symptoms, such as overt leg extension, weak walking, twisted hindpaw and stiff hindlimb, and complete infantile lethality. However, it is not clear if the overt dystonic symptoms were caused by the neurodegeneration in the dying N-CKO mice. Here, the effects of improved maternal care and nutrition during early life on the symptoms in N-CKO mice were analyzed by culling the litter and putting wet food to examine whether the overt dystonic symptoms and severe lack of weight gain are caused by malnutrition-related neurodegeneration. Although the N-CKO mice in this study replicated the severe lack of weight gain and overt "dystonic" symptoms during the lactation period regardless of culling at postnatal day zero or later, there was no significant difference in the brain astrocytes and apoptosis between the N-CKO and control mice. Moreover, more than half of the N-CKO mice with culling survived past the lactation period. The surviving

[1]Corresponding author: Dr. Yuqing Li, Department of Neurology, College of Medicine, University of Florida, PO Box 100236, Gainesville, FL 32610-0236, USA, Tel.:1-352-273-6546; Fax: 1-352-273-5989, yuqingli@ufl.edu.

Current Address: Fangfang Jiang: Department of Pharmacology and Therapeutics, College of Medicine, University of Florida, 1200 Newell Drive, ARB R5-126, Gainesville, Florida, 32610 USA

Current Address: Kelly Dexter: Florida Museum of Natural History, University of Florida, Powell Hall, 3215 Hull Road, Gainesville, Florida, 32611-2710 USA

Current Address: Bryan Salvato: Florida State University College of Medicine, 1115 West Call Street, Tallahassee, Florida 32306-4300 USA

Contributors

FY, FJ, KD, and BS performed experiments. FY and YL designed the experiments, analyzed the data, and wrote the manuscript.

Author Statement

Fumiaki Yokoi: Conceptualization, Investigation, Formal analysis, Writing - Original Draft, Funding acquisition. **Fangfang Jiang**: Investigation. **Kelly Dexter**: Investigation. **Bryan Salvato**: Investigation. **Yuqing Li**: Conceptualization, Formal analysis, Writing - Review & Editing, Funding acquisition

Appendix Fig. 1

(**A**) A representative immunohistochemical image of a CT (*Nestin-cre*+/− *Dyt1 loxP*+/−) mouse brain slice stained with anti-GFAP antibody and DAB. (**B**) A negative control image of the brain slice from the same mouse without primary antibody. The images were taken with 2.5× objective lens. The scale bars indicate 1 mm.

adult N-CKO mice did not display overt “dystonic” symptoms, whereas they still showed small body weight. The results suggest that the overt “dystonic” symptoms in the N-CKO mice were independent of prominent neurodegeneration, which negates the role of neurodegeneration in the pathogenesis of DYT1 dystonia.

Keywords

Dystonia; DYT1; *Nestin-cre*; Neurodegeneration; *Tor1a*; torsinA

1. Introduction

DYT1 early-onset generalized torsion dystonia (dystonia 1: OMIM: #128100) is a hereditary movement disorder characterized by abnormal torsion posture and repeated movements without apparent neurodegeneration [1]. The symptoms initially affect the limbs in childhood or adolescence and often become generalized [2]. The symptoms can vary depending on the patients [3]. DYT1 dystonia is mainly the result of a heterozygous in-frame trinucleotide deletion (ΔGAG) in *DYT1/TOR1A*, resulting in a glutamic acid loss in torsinA, with 30–40% penetrance [4]. Other mutations in the gene were also reported in rare cases [5–8]. Moreover, a two-month-old boy with a homozygous nonsense mutation in the gene showed severe arthrogryposis, developmental delay and dystonic movements [9].

Heterozygous *Dyt1/Tor1a* ΔGAG knock-in (*Dyt1* KI) mice, which have the corresponding trinucleotide deletion, exhibit long-term depression (LTD) deficits in the cortico-striatal pathway [10], abnormal sustained co-contractions of agonist and antagonist muscles [11], and motor deficits in the hindlimbs during the beam-walking test [12], which are ameliorated by trihexyphenidyl, one of the frontline treatments for DYT1 dystonia [10, 11]. Motor deficits were also reported in another line of KI mice [13], suggesting that the motor deficits were reproducible in these independent lines. Although the *Dyt1* KI mice have subtle anatomical alterations in the amygdala and cerebellum [12, 14, 15], they do not have apparent neurodegeneration. The *Dyt1* ΔGAG mutation may cause a partial loss of torsinA function [16–18]. Moreover, both the heterozygous *Dyt1* KI mice and the heterozygous *Dyt1* KO mice exhibit deficits in the presynaptic release [19, 20] and abnormal brain metabolism as detected by brain imaging [21, 22]. Both the heterozygous *Dyt1* KO mice [20] and the *Dyt1* knock-down (KD) mice [23] show motor deficits similar to the heterozygous *Dyt1* KI mice. Moreover, the cerebral cortex-, the striatum-, the cholinergic cell-, and the dopamine receptor 2-expressing-cell-specific *Dyt1* conditional KO mice (cKO, sKO mice, ChKO, d2KO, respectively) show motor deficits [24–27]. On the other hand, the cerebellar Purkinje cell-specific *Dyt1* conditional KO in both the wild-type and the KI background show improved motor performance [28], suggesting that torsinA loss in distinct neurons affects motor performance differently. Motor deficits without overt dystonic symptoms were also reported in other genetic mouse models [29, 30], such as models for DYT11 [31, 32], DYT12 [33], and DYT25 dystonia [34]. Moreover, the homozygous *Dyt1* KI mice show neonatal lethality [12, 35]. Similarly, the homozygous *Dyt1* KO mice cannot suckle milk and die soon after birth [24].

In contrast with the heterozygous *Dyt1* KI, *Dyt1* cKO, and *Dyt1* sKO mice, which show mild motor deficits without obvious neurodegeneration, several other mutant and transgenic mouse models show neurodegeneration and overt “dystonic” symptoms. An example is the forebrain-specific Dlx-CKO mouse, which has a heterozygous *Tor1a*/*Dyt1* knockout (KO) in one allele and *Dlx5/6-Cre*-mediated conditional KO in the other [36], exhibits a selective loss of dorsolateral striatal cholinergic interneurons and overt “dystonic” symptoms. However, *Dyt1* d2KO mice show a decreased number of striatal cholinergic interneurons and motor deficits without overt “dystonic” symptoms, suggesting that the decreased number of striatal cholinergic interneurons itself does not cause overt “dystonic” symptoms [27]. Moreover, cerebellar microinjection of AAVs expressing shRNAs against torsinA mRNA induces abnormal firing of cerebellar neurons, neuronal death within the deep cerebellar nuclei, and overt “dystonic” symptoms [37].

Additionally, an N-CKO mouse model presents severe growth retardation, neurodegeneration, overt “dystonic” symptoms, such as overt leg extension, weak walking, twisted hindpaw and stiff hindlimb, and complete infantile lethality by postnatal day 16 (P16) [38]. In the deep layers of the sensorimotor cortex, ventral posterior thalamus, globus pallidus (GP), deep cerebellar nuclei (DCN), red nucleus (RN), and facial nerve nucleus (7N), immunohistochemistry with antibodies against either Glial Fibrillary Acidic Protein (GFAP), an intermediate filament protein composing cytoskeleton in astrocytes [39], and Cleaved-Caspase-3 (CC3), a marker for apoptosis, shows that the N-CKO mice at P10 have increased neurodegeneration and apoptosis, respectively. However, the contributions of the increased astrocytes and CC3-expressing cells detected in the N-CKO mouse brains to the overt “dystonic” symptoms are questionable because the N-CKO mice were moribund, presumably had multiple organ failures and tissue deterioration. The smaller N-CKO mice may suffer malnutrition, due to their disadvantage in the competition for milk with their larger littermates and resultant poor-nursing, and then exhibit neurodegeneration and die. Here, the effects of improved maternal care and nutrition during early life on the symptoms in the N-CKO mice were analyzed by culling the newborn litters and putting wet food on the cage floor.

2. Materials and methods

2.1. Generation of N-CKO mice

All experiments were conducted in compliance with the USPHS Guide and approved by the University of Florida Institutional Animal Care and Use Committee. Mice were housed with *ad libitum* access to food and water under the condition of 12 hours-light and 12 hours-dark. Wet food was also put on the cage floor to facilitate accessing the food. *Dyt1 loxP* −/− female mice, which have floxed *Dyt1* exons 3–4, were prepared as previously described [24]. Recombination between these two *loxP* sites leads to the loss of torsinA expression [16]. Heterozygous *Dyt1* KO (*Dyt1* +/Δ) mice were prepared from the *Dyt1 loxP* mice as previously described [24]. *Nestin-cre* +/− mice [40] were obtained from the Jackson lab [B6.Cg-Tg(Nes-cre)1Kln/J, Strain 003771]. *Nestin-cre* mice can delete the floxed gene in neurons and glial cells. *Nestin-cre* +/− *Dyt1* +/Δ male mice were obtained from crossing *Nestin-cre* +/− and *Dyt1* +/Δ mice. *Nestin-cre +/− Dyt1 +/*Δ male mice were then crossed

with *Dyt1 loxP* −/− female mice to generate *Nestin-cre* +/− *Dyt1 loxP* −/Δ (N-CKO) mice and control (CT) littermates. *Nestin-cre* genotype was identified by PCR with the primer set specific for *Nestin-cre* (Nestin-5: 5'-CCGCTTCCGCTGGGTCACTGT-3'; Nestin-2: 5'-CTGAGCAGCTGGTTCTGCTCCT-3'; Nestin-3: 5'-GACCGGCAAACGGACAGAAGCA-3'). *Dyt1* Δ, *Dyt1 loxP*- and *Dyt1*+ loci were genotyped as previously described [24].

2.2. Western blot analysis

Brain, liver, heart and spinal cord were dissected from N-CKO (n=2) mice and CT littermates (*Dyt1 loxP* +/−; n=2) from a litter at P0 and homogenized in ten volume of ice-cold lysis buffer [16]. Brains were homogenized in glass Dounce tissue grinders (7ml; Kontes) with 20 strokes. Livers and spinal codes were homogenized with a Pellet pestle motor (Kontes) for 30 sec. Hearts were homogenized with tissue tearor (Biospec Products, Inc.) for 30 sec. Each homogenate was sonicated, and the proteins were extracted in 1% Triton X-100 lysis buffer as previously described [16]. Protein concentration was measured by Bradford assay [41] with Bio-rad protein assay dye reagent concentrate and bovine serum albumin as a standard. Twenty μg of the protein extract was used for 10% sodium dodecyl sulfate polyacrylamide gel electrophoresis and transferred onto Millipore Immobilon–FL transfer PVDF membranes. The membranes were washed with 0.1 M phosphate-buffered saline and processed as previously described [42]. After blocking the membrane in LI-COR Odyssey blocking buffer, torsinA and calnexin levels were detected with a combination of rabbit anti-torsinA antibody (Abcam, ab34540; 1:1,000 dilution) and IRDye 680RD donkey anti-rabbit IgG (H+L) (LI-COR, 926–68073; 1:15,556 dilution), and a combination of mouse anti-calnexin antibody (Chemicon, MAB3126; 1:1,000 dilution) and IRDye 800CW donkey anti-mouse IgG (H+L) (LI-COR, 926–32212; 1:15,556 dilution), respectively. The signals were captured with an LI-COR Odyssey imaging system and analyzed with Image Studio Lite Ver. 5.2. TorsinA/calnexin signal ratio of N-CKO mice was normalized to that of *Dyt1 loxP+/−* mice and expressed in percentage.

2.3. Genotyping of N-CKO mice without culling

To analyze the survival ratio of N-CKO mice without culling at around weaning age, N-CKO mice and their CT littermates were generated according to the breeding scheme shown in Figure 1A. Eighteen pups were obtained from two litters, and their tails were cut at P7 for genotyping. Other seventeen pups from 4 litters were alive at weaning age of P21. Their tails were cut at around two weeks of age for genotyping. PCR was performed as described above to genotype the two batches.

2.4. Growth and survival analysis of N-CKO mice with culling

Body weights were measured in two other batches of N-CKO and CT littermates with culling. In the first batch, four pups were randomly selected from each litter without genotyping and marked with tattoo ink at P0. Thirty-six pups were selected from 9 litters at P0 and returned to their mothers. Six pups died, and their bodies were lost before genotyping, and therefore they were removed from growth analysis. The remaining 30 pups were genotyped [N-CKO (n=6; 5 males; 1 female), *Nestin-cre* +/− *Dyt1 loxP* +/− (n=6; 4 males; 2 females), *Dyt1 loxP* −/Δ (n=8; 3 males; 5 females), and *Dyt1 loxP* +/− (n=10; 2

males; 8 females) from nine litters] and their body weights were monitored daily (longest cutoff at P74). Two N-CKO (n=2; 1 male at P11; 1 female at P11), three *Nestin-cre* +/− *Dyt1 loxP* +/− mice (n=3; 1 male at P14; 2 females at P58, P66), four *Dyt1 loxP* −/Δ mice [n=4; 4 females at P11, P58, P65, P66], and six *Dyt1 loxP* +/− mice [n=6; 2 males at P43, P65; 4 females at P40, P65 (n=2), P66] were removed from the study at the indicated ages. The pups were weaned at P21. Representative movies were taken at P10 for some of these pups.

The second batch of 39 mice was generated from five litters in the same breeding scheme. The second batch of mice was genotyped during the early lactation period before culling. The batch consisted of N-CKO (n=13; 10 males; 3 females), *Nestin-cre* +/− *Dyt1 loxP* +/− (n=8; 5 males; 3 females), *Dyt1 loxP* −/Δ (n=7; 1 male; 6 females), and *Dyt1 loxP* +/− (n=11; 6 males; 5 females) mice before culling. Extra control littermates were removed after P9 to increase the access of N-CKO mice to their mother. Three *Nestin-cre* +/− *Dyt1 loxP* +/− mice (n=3; 3 males at P9, P10, P13), five *Dyt1 loxP* −/Δ mice [n=5; 1 male at P13; 4 females at P9 (n=1) and P10 (n=3)], and three *Dyt1 loxP* +/− mice (n=3; 1 male at P13; 2 females at P20) were removed. The pups were weaned at P21. Moreover, one *Nestin-cre* +/− *Dyt1 loxP* +/− mouse (n=1; 1 female at P47), two *Dyt1 loxP* −/Δ mice (n=2; 2 females at P47), and three *Dyt1 loxP* +/− mice (n=3; 1 male at P26; 2 females at P47) were removed. The body weight of this batch was measured for 90 days (cutoff at P47 for *Dyt1* +/Δ).

2.5. Immunohistochemistry with GFAP and CC3 antibodies

N-CKO and CT mice were prepared as described above with or without culling at P0. To produce the first group of mice with culling, extra littermates were removed at P0, and four mice were maintained in each litter until P10. Moreover, a wild-type (WT) mouse at P10 was prepared as an additional CT mouse. To produce the second group of mice without culling, another litter was generated and kept with their mother until P10 without culling or additional wet food on the floor. The first group, which consists of N-CKO (n=3) and control (n=3; *Dyt1 loxP* −/Δ, *Nestin-cre*+/− *Dyt1 loxP*+/−, and WT) mice, and the second group, which consists of N-CKO (n=2) and control [n=5; *Dyt1 loxP*+/− (n=3), *Dyt1 loxP* −/Δ (n=1), *Nestin-cre*+/− *Dyt1 loxP*+/− (n=1)] mice, were deeply anesthetized and perfused with 0.1 M phosphate buffer (PB; pH 7.4) and following 4% paraformaldehyde/0.1 M PB. The brains were dissected and put in 4% paraformaldehyde, 0.1 M PB overnight. The brains were put in 30% sucrose/0.1 M PB until the brains sunk to the bottom. The brains were frozen with dry ice powder and sliced sagittally with a Histoslide 2000 sliding-microtome (Reichert-Jung) at 30 μm thickness. Every other sixth slice was analyzed for each brain. Twelve slices were selected among them for each brain and blocked with serum according to the manufacturer's instruction (Vectastain). The twelve slices from each genotype were treated with rabbit polyclonal GFAP antibody (Dako; Cat. No. Z0334; 1:1,000 dilution). Another set of slices were prepared and treated with serum and rabbit monoclonal Cleaved Caspase-3 (Asp175) (5A1E) antibody (Cell Signaling; Cat. No. #9664; 1:100 dilution). As a negative control, four brain slices from a *Nestin-cre*+/− *Dyt1 loxP*+/− mouse were treated with the blocking serum without primary antibody. All slices were then treated with Vectastain ABC kit for peroxidase rabbit IgG and DAB substrate (Vector; SK-4100). The brain slices were mounted on Superfrost/Plus microscope slides (Fisher Scientific) and dried overnight, and then covered with Permount (Fisher Scientific) or DPX (Fluka) and cover

glasses. The representative images were captured with a Zeiss Axiophot RZGF-1 microscope [10× (for the samples) or 2.5× (for the negative control) plan-NEOFLUAR objective lens] and Neurolucida program (MBF Bioscience). GFAP-expressing cells or CC3-expressing cells were examined in the hippocampus, cerebellum, and six sensorimotor regions, *i.e.*, cerebral sensorimotor cortex, ventral posterior thalamus, globus pallidus (GP), deep cerebellar nuclei (DCN), red nucleus (RN) and facial nerve nucleus (7N). Each stained region was evaluated as level 0 (no positive cells), 1 (a few positive cells), 2 (moderate numbers of positive cells), or 3 (many positive cells) and the maximal level of the region among the examined slices in each mouse was used for the analysis by a nonparametric statistics.

2.6. Statistics

Statistical analysis was performed with the R program version 3.5 in most cases except the proportional hazards model for survival analysis, which was analyzed by the SAS program. Student's t-test was used to analyze western blot data. Fisher's exact test was used to analyze the numbers of the surviving mice and the mice showing obvious dystonic symptoms. Analysis of variance was used to compare body weights in the growth curves. Paired and Welch's t-tests were used to compare the growth rates before and after weaning for the first batch culling at P0 and the second batch with culling later (after P9), respectively. Kaplan-Meier curve was used to plot the survival ratio. The body weights of the mice at P10 without culling or putting additional wet food on the floor were compared by using a R liner mixed model (lm) concerning genotype and sex. Wilcoxon rank sum test was used to analyze the immunohistochemistry. Significance was assigned at $p < 0.05$.

3. Results

3.1. Generation of N-CKO mice

Nestin-cre +/− *Dyt1* +/Δ male mice were crossed with *Dyt1 loxP* −/− female mice to generate *Nestin-cre* +/− *Dyt1 loxP* −/Δ (N-CKO) mice and CT littermates including *Nestin-cre* +/− *Dyt1 loxP* +/−, *Dyt1 loxP* −/Δ, and *Dyt1 loxP* +/− mice (Figure 1A). The pups were genotyped by PCR with tail DNA, and the primer sets specific for *Nestin-cre*, *Dyt1* Δ, *Dyt1 loxP*- and *Dyt1* wild type (+) loci (Figure 1B). The torsinA and calnexin levels in the brain, spinal cord heart, and liver were measured in N-CKO and CT (*Dyt1 loxP+/−*) littermates at P0 (Figure 1C, n=2 each). The torsinA levels normalized to calnexin were significantly reduced in the brain and spinal cord of N-CKO mice compared to those of CT mice (means ± standard errors; brain: CT: 100 ± 11 %; N-CKO: 13 ± 5 %; p= 0.019; spinal cord: CT: 100 ± 3 %; N-CKO: 14 ± 2 %; p= 0.0019; Figure 1D). On the other side, the normalized torsinA levels in the heart and liver of N-CKO mice were reduced to approximately half of those in the CT mice, as predicted from the heterozygous KO in these tissues (heart; CT: 100 ± 5 %; N-CKO: 45 ± 2 %; p= 0.010; liver; CT: 100 ± 6 %; N-CKO: 42 ± 1 %; p= 0.012; Figure 1D).

3.2. Infant lethality, overt dystonic symptoms, and lack of weight gain in N-CKO mice without culling

Mice were generated according to the breeding scheme shown in Figure 1A. Eighteen pups were obtained from two litters and their tails were cut at P7 and genotyped [n=18; N-CKO (n=7), *Nestin-cre* +/− *Dyt1 loxP* +/− (n=6), *Dyt1 loxP* −/Δ (n=4), *Dyt1 loxP* +/− (n=1)]. The other seventeen pups from 4 litters were surviving at weaning age of P21. Their tails were cut around 2 weeks of age for genotyping [n=17; N-CKO (n=0), *Nestin-cre* +/− *Dyt1 loxP* +/− (n=8), *Dyt1 loxP* −/Δ (n=7), *Dyt1 loxP* +/− (n=2)]. The surviving mouse ratios of N-CKO mice versus CT mice, which include all three control genotypes, were significantly different between two batches (p=0.0076). The results suggest that N-CKO mice die before weaning age. This is reminiscent of the complete lethality by P16 as reported in another line of N-CKO mice (n=25) [38].

Consistent with the earlier report, small body size and overt “dystonic” symptoms, such as explicit leg extension, weak walking, twisted hindpaw and stiff hindlimb, were observed in all the N-CKO mice. These obvious symptoms were only shown in N-CKO mice, and therefore the appearance of these symptoms was significantly high in N-CKO mice (P7; CT: n=11; N-CKO: n= 7; $p=3.1 \times 10^{-5}$) and suggests that these phenotypes were reproduced in the current N-CKO mouse line. The small N-CKO mice were easily outcompeted by their control littermates and had difficulty gaining access to the mother; stayed away from the mother without nursing and died. This observation hinted that the complete neonatal lethality of the small N-CKO mice might be a consequence of malnutrition due to the disadvantage in the competition for milk with their larger littermates.

3.3. Improved survival of N-CKO mice by culling

To examine if an improvement in nutrition and nursing from birth attenuates the symptoms in N-CKO mice, the pup numbers were reduced by culling the litters. Four pups were randomly selected from each litter and left with their mother at P0, and wet food was provided continuously on the cage floor. A total of 30 pups [N-CKO mice (n=6), *Nestin-cre* +/− *Dyt1 loxP*+/− (n=6), *Dyt1 loxP*−/Δ (n=8), and *Dyt1 loxP*+/− (n=10)] from nine litters were weighed until P74. There was a trend, but no significant difference, in their body weight at P0 (p=0.075; Figure 2A). N-CKO mice were significantly underweight from P4 (P4: p=0.024; Figure 2A) to P66 (P66: p=0.049; Figure 2B). The lactation period in this study was defined as the postnatal period before weaning the pups at P21. There was no significant difference between the growth rate before (P0 to P21; n=3; mean ± standard error: 0.13 ± 0.00 g/day) and after the weaning (P22 to P43; n=3; 0.27 ± 0.06 g/day, p=0.12) in N-CKO mice. Moreover, there was no significant difference in the survival ratios among the four genotypes (p=0.8; Figure 2C).

To examine whether litter culling during the lactation period is enough to increase the survival ratio of the N-CKO mice, pups from other litters were genotyped during the early lactation period, and extra CT littermates were removed after P9. Wet food was put on the floor to support the nutrition of the pups. Consistent with the above observations, there was a trend, but no significant difference in body weight at P0 [N-CKO mice (n=13), *Nestin-cre*+/− *Dyt1 loxP*+/− (n=8), *Dyt1 loxP*−/Δ (n=7), and *Dyt1 loxP*+/− (n=11) from five litters;

p=0.052; Figure 2D]. Extra CT littermates were removed from P9 to P47 to improve the survival of the N-CKO mice. The N-CKO mice presented as significantly underweight from P2 (p=0.0004; Figure 2D) to P90 (p=0.0009; Figure 2E). There was a significant increase of the growth rate after the weaning (P0 to P21; n=10; mean ± standard error: 0.11 ± 0.01 g/day vs P22 to P43; n=9; 0.40 ± 0.02 g/day; $p=3.7\times10^{-7}$), suggesting that lower body weight in the N-CKO mice during the lactation period was more acute, although low body weight continued into adulthood. Moreover, there was a significant difference in the survival ratios among the four genotypes (p = 0.014; Figure 2F).

The body weights described above were further compared between the two batches of N-CKO mice from P0 to P10 (Figure 2G). Although there were significant differences in the body weights between these batches at P6 (p=0.036) and P7 (p=0.022), there was no significant difference at other ages (p>0.05). Moreover, the growth curves between the two batches of N-CKO mice after P10 showed no significant difference (p>0.05; Figure 2H). The results suggest that low body weight during the examined period was not influenced by the timing of the culling.

In addition to the survival ratios between the N-CKO mice and CT mice shown in Figure 2C and 2F, the actual numbers of N-CKO mice in both batches are plotted in Figure 2I. Two out of four N-CKO mice (50%) in the first batch with culling at P0 survived during the observed period up to P74, which is in contrast to the complete lethality by P16 in the previously reported N-CKO mice (n=25) [38]. Since two N-CKO mice were removed from monitoring at P11, the percentage of survived mice was calculated without them. The survival ratio of N-CKO mice was significantly improved compared to the prior reported case (p=0.015). Moreover, nine out of thirteen N-CKO mice (69%) in the second batch, with culling occurring later, survived during the observed period up to P90 in contrast to the lethality previously reported in N-CKO mice (n=25) [38]. The survival ratio of N-CKO mice was also significantly improved compared to the prior reported case ($p=4.4\times10^{-6}$). Overall, eleven out of seventeen N-CKO mice (65%) in the two batches with culling survived during the observed periods. Since all N-CKO mice without culling are supposed to die before weaning as shown in 3.2, the survival ratio of the N-CKO mice with culling in this study can be estimated to be significantly improved ($p=8.7\times10^{-5}$). The results suggest that the improvement of nutrition and nursing during the lactation period increased the survival ratio of the N-CKO mice.

3.4. Overt “dystonic” symptoms during the lactation period in N-CKO mice with culling

The overt “dystonic” symptoms were also observed in all examined N-CKO mice with the culling of littermates at P0 in the first batch shown in Figure 2A–C [Supplemental movies were taken at P10; 1: CT (*Dyt1 loxP*−/Δ) mouse; 2: N-CKO mouse from a batch with culling at P0]. Moreover, the overt “dystonic” symptoms were observed in all examined N-CKO mice with culling occurring later as shown in Figure 2D–F. The overt “dystonic” symptoms were not observed in the surviving adult N-CKO mice in both batches. The numbers of obvious dystonic mice between the N-CKO and CT mice were compared in both infantile (P10) and adult (P60) ages for each batch. In the first batch with culling at P0, all N-CKO mice (n=5) showed overt dystonic symptoms, and no CT mice (n=23) showed overt dystonic

symptoms at P10. The appearance of overt dystonic symptoms was significantly high in N-CKO mice (p=1.0 × 10^{-5}). On the other hand, no N-CKO (n=2) and CT (n=16) mice showed overt dystonic symptoms at P60 (p=1). In the second batch with culling later, all N-CKO mice (n=13) showed overt dystonic symptoms, and no CT mice (n=24) showed overt dystonic symptoms at P10. The appearance of overt dystonic symptoms was significantly high in N-CKO mice (p=2.8 × 10^{-10}). Significantly, no N-CKO (n=9) and CT (n=9) mice showed overt dystonic symptoms at P60 (p=1). These results suggest the appearance of overt "dystonic" symptoms during the lactation period only in N-CKO mice, regardless of culling at P0 or later, and significant improvement of overt dystonic symptoms in the surviving adult N-CKO mice in both batches.

3.5. No evident changes of neurodegeneration or apoptosis in N-CKO mouse brains with culling

Brains from CT (n=3) and N-CKO (n=3) mice with culling at P0 were stained at P10 with a GFAP antibody to examine the distribution of astrocytes in the six sensorimotor regions, the hippocampus, and the cerebellum (Figure 3). There was no significant difference between N-CKO mice and CT mice in the appearance of the GFAP-positive cells in each brain region, *i.e.*, cerebral cortex (median level: CT: 1, N-CKO: 2; p=0.62; Figure 3A, B), thalamus (CT: 1, N-CKO: 1; p=0.30; Figure 3C, D), GP (CT: 2, N-CKO: 2; p=0.81: Figure 3E, F), DCN (CT: 2, N-CKO: 2; p=1: Figure 3G, H), RN (CT: 1, N-CKO: 1; p=0.30; Figure 3I, J), and 7N (CT: 2, N-CKO: 3, p=0.19; Figure 3K, L). GFAP-positive cells in the hippocampus and cerebellum were also observed in both CT and N-CKO mice (Figure 3M–P). Overall, there was no obvious difference between CT and N-CKO mice in the appearance of GFAP-positive cells in any of the brain regions examined, in contrast with the previous report [38]. The present results are consistent with another report showing a broad distribution of GFAP-expressing cells in the mouse brain [43] and multiple previous studies showing astrogenesis during the lactation period [44]. The results also suggest that the detected astrocytes in both genotypes were generated as part of the normal brain developmental process.

Brain sections from the same set of mice with culling at P0 were also stained with CC3 antibody to examine whether N-CKO mice exhibit increased apoptosis. However, very few CC3-positive cells were detected in both genotypes (Figure 4). There was no significant difference between N-CKO and CT mice in the appearance of CC3-positive cells in each brain region, *i.e.*, cerebral cortex (median level: CT: 0, N-CKO: 0; p=0.51; Figure 4A, B), thalamus and GP (CT: 0, N-CKO: 0; p=NA: no positive cell in both genotypes; Figure 4C–F), DCN (CT: 1, N-CKO: 0; p=0.20; Figure 4G, H), RN (CT: 0, N-CKO: 0; p=0.51, Figure 4I, J), and 7N (CT: 1, N-CKO: 1; p=0.68; Figure 4K, L). The representative immunohistochemical images with anti-CC3 antibody in the hippocampus and cerebellum are also shown (Figure 4M–P). Contrary to the previous report [38], the results suggest that N-CKO mice with culling at P0 did not show increased apoptosis at P10.

3.6. No significant changes of neurodegeneration or apoptosis in N-CKO mouse brains without culling

Another batch of N-CKO and CT mice without culling was prepared by the same breeding scheme and fed only by their mother without special treatments such as culling or putting additional wet food on the floor. N-CKO mice without culling showed small body size, abnormal movements, and died during eary infant age. The body weights of survifing N-CKO and CT mice from a litter without culling were measured at P10. The N-CKO mice were significantly lighter than CT mice (mean ± SE; CT: n=5, 7.02 ± 0.19 g; N-CKO: n=2, 2.55 ± 0.10 g; p=0.00034).

Distributions of astrocytes and apoptotic cells in the corresponding brain regions were examined at P10 between N-CKO and CT mice from the litter without culling. The brains were stained with GFAP antibody, and the six sensorimotor regions, the hippocampus and the cerebellum were examined (Figure 5). GFAP-positive cells were detected in these multiple brain regions regardless of the genotype. There was no significant difference between N-CKO mice and CT mice in the appearance of the GFAP-positive cells in each brain region, *i.e.*, cerebral cortex (median level: CT: 3, N-CKO: 2.5; p=1; Figure 5A, B), GP (CT: 2, N-CKO: 2.5; p=0.62: Figure 5E, F), DCN (CT: 2, N-CKO: 1.5; p=0.21: Figure 5G, H), RN (CT: 2, N-CKO: 2; p=0.46; Figure 5I, J), and 7N (CT: 2, N-CKO: 2, p=NA because all compared data were same; Figure 5K, L). On the other hand, there was a trend of increased GFAP in the thalamus of N-CKO mice, but it was not statistically significant (CT: 1, N-CKO: 3; p=0.052; Figure 5C, D). GFAP-positive cells in the hippocampus and cerebellum were also observed in both CT and N-CKO mice (Figure 5M–P). Overall, there was no significant difference between CT and N-CKO mice in the appearance of GFAP-positive cells in the most of the examined brain regions, in contrast with the previous report [38]. The present results are mostly consistent with the CT and N-CKO mice with culling as described above. The results suggest that the detected astrocytes in both genotypes were generated as part of the normal brain developmental process.

Brain sections from the same set of mice without culling were also stained with CC3 antibody to examine whether N-CKO mice exhibit specific apoptosis or not. CC3-positive cells were detected in both genotypes (Figure 6). There was no significant difference between N-CKO and CT mice in the appearance of CC3-positive cells in each brain region, *i.e.*, cerebral cortex (median level: CT: 2, N-CKO: 2; p=0.46; Figure 6A, B), thalamus (median level: CT: 1, N-CKO: 1.5; p=0.19; Figure 6C, D), GP (CT: 1, N-CKO: 1; p=0.46; Figure 6E, F), DCN (CT: 2, N-CKO: 2; p=NA; Figure 6G, H), RN (CT: 2, N-CKO: 2; p=NA; Figure 6I, J), and 7N (CT: 1, N-CKO: 2; p=0.26; Figure 6K, L). The representative immunohistochemical images with anti-CC3 antibody in the hippocampus and cerebellum are also shown (Figure 6M–P). CC3-positive cells were detected in both genotypes at similar levels. Contrary to the previous report [38], the results suggest that N-CKO mice did not show significantly increased apoptosis at P10.

Finally, the detection of GFAP or CC3-positive cells were verified using the brain slices treated without primary antibody (Appendix Fig. 1).

Since both CT mice and N-CKO mice showed similar distributions of the GFAP and CC3-positive cells in most of the examined brain regions at P10 regardless of culling or not, the GFAP-positive cells in both mice were most likely the astrocytes generated by normal astrogenesis during development, and not the glial scar of neurodegeneration. On the other hand, a trend of increased GFAP was observed in the thalamus of N-CKO mice without culling, but not in N-CKO mice with culling. The trend of increased GFAP may be related to the starvation caused by the disadvantage of smaller N-CKO mice without culling in competing against bigger CT mice because thiamine deficiency induces thalamic neurodegeneration in mice [45]. Since N-CKO mice showed abnormal postures regardless culling or not, the overt dystonic symptoms was likely not caused by neurodegeneration of thalamus.

4. Discussion

Consistent with the previous N-CKO mouse line [38], the present N-CKO mice showed lower body weight and infant lethality before weaning age. Moreover, the N-CKO mice with culling and control mice in this study showed the same distribution of astrocytes as reported in another line of N-CKO mice, suggesting that the detected astrocytes were most likely generated by astrogenesis rather than glial scars generated by neurodegeneration. Additionally, CC3-positive apoptotic cells were scarcely detected in both N-CKO mice with culling and CT mice, suggesting no significant increase of apoptotic cells in N-CKO mice with culling. Consistently, there was no significant difference in the distributions of astrocytes and CC3-positive apoptotic cells between N-CKO and CT mice without culling at P10. In this study, the N-CKO mice regardless of culling or not showed dystonic symptoms without alterations of distributions of astrocytes and apoptotic cells in the brains, suggesting that the dystonic symptoms were not directly related to prominent neurodegeneration. These neurodegeneration-independent “dystonic” symptoms are consistent with clinical studies of DYT1 dystonia in humans [46]. Finally, low body weight and overt “dystonic” symptoms, such as overt leg extension, weak walking, twisted hindpaw and stiff hindlimb as reported in another line of N-CKO mice [38], were reproduced in the present N-CKO mouse line during the lactation period, regardless of culling at P0 or later. These results suggest that these phenotypes are related to the pan-neuronal and glial KO of *Dyt1/Tor1a* with combination of heterozygous KO in the whole body.

In contrast to the reported case [38], the present study N-CKO mice and CT mice showed the same distribution of GFAP-positive cells in the corresponding brain regions at P10 regardless of culling or not. This suggests that the astrocytes detected in the N-CKO mice were generated by astrogenesis during the developmental step [44, 47–52] rather than glial scars generated by reactive astrogliosis after brain injury [39, 53] or neurodegeneration [54]. Since N-CKO mice showed overt dystonic symptoms and severe lack of weight gain without significant increase of GFAP-expressing cells in the specific brain regions, the overt dystonic symptoms and severe lack of weight gain in N-CKO mice were not accompanied by brain-region-specific neurodegeneration, at least in the present study. Although both the reported and the present N-CKO mice seem to have some malnutrition during the lactation period, it is known that malnutrition does not affect astrogliosis in many cases. For example, GFAP expression is not influenced by protein malnutrition during the developmental stage in rats

[55]. Furthermore, protein malnutrition affects cerebellar development without alteration of GFAP expression [56]. It should be noted that a subtle alteration of GFAP expression in the suprachiasmatic nucleus was reported with malnutrition during rat brain development [57] and neurodegeneration is induced by thiamine deficiency in mice [45]. Since the present N-CKO mice regardless of culling or not showed the same distribution of GFAP-positive cells observed in CT mice, malnutrition in these N-CKO mice seems mostly not to affect GFAP expression in the brain except thalamus. Because thiamine deficiency induces thalamic neurodegeneration in mice [45], the trend of increased GFAP may be related to the starvation and thiamine deficiency caused by the disadvantage of smaller N-CKO mice without culling in competing against bigger CT mice.

In contrast to the brain-region-specific increases of CC3-positive cells in the previously reported N-CKO mice [38], the present study N-CKO mice regardless of culling or not did not show brain-region-specific increases of CC3-positive cells. Therefore, overt dystonic symptoms and severe lack of weight gain were not accompanied by the brain-region-specific apoptosis, at least in the present N-CKO mice. The results suggest that the increased CC3-positive cells in the N-CKO mice of the previous study may not directly relate to the overt dystonic symptoms, but rather to the dying process.

Here, wet food was added on the floor to support nutrition for the pups which had difficulty getting milk. Culling and putting wet food on the floor should improve nutrition for the pups. In addition to nutrition, increased mother-offspring interaction also could have played a role to rescue pups from complete lethality before weaning. The complete infantile lethality in N-CKO mice seems to be attenuated by culling and providing wet food on the cage floor, which suggests that the complete lethality may be an artefact caused by the failure of the pups to get enough milk and nutrition, and inadequate nursing. The lethality in N-CKO mice resembles *Dyt1* KO mice, which have no milk in their stomachs and die on the day of birth [24]. Significant loss of torsinA seems to lead to malnutrition because of the pups' inability to latch and suckle milk from the mother. After weaning, the N-CKO mice with culling significantly gained weight accompanied by the disappearance of the overt "dystonic" symptoms, suggesting that these symptoms before weaning were likely affected by malnutrition and poor-nursing during the lactation period, which does not commonly occur in DYT1 dystonia patients. Taken together, the results support neither the N-CKO mice as an appropriate model nor neurodegeneration as the pathogenesis of DYT1 dystonia.

5. Conclusion

Although torsinA hypofunction mice exhibited severe lack of weight gain and overt "dystonic" symptoms without obvious neurodegeneration, these symptoms were improved by nutrition and nursing. Since obvious neurodegeneration was not detected, the results suggest that the overt dystonic symptoms observed in the N-CKO mice were most likely not caused by neurodegeneration.

Supplementary Material

Refer to Web version on PubMed Central for supplementary material.

Acknowledgements

We thank UF ACS staff, Jareisha Vickers, Aysha Awal, Yuning Liu, and Professor Maurice S. Swanson. This work was supported by Tyler's Hope for a Dystonia Cure, Inc., NIH (NS37409, NS47466, NS47692, NS54246, NS57098, NS65273, NS72782, NS74423, NS 75012, NS82244), Bachmann-Strauss Dystonia and Parkinson Foundation, Inc., and DOD (W81XWH1810099).

Footnote

FY was partially supported by Office of the Assistant Secretary of Defense for Health Affairs through the Peer Reviewed Medical Research Program Discovery Award under Award No. W81XWH1810099. Opinions, interpretations, conclusions, and recommendations are those of the author and are not necessarily endorsed by the Department of Defense.

Abbreviations

CC3	Cleaved-Caspase-3
CT	control
DCN	deep cerebellar nuclei
Dlx-CKO mouse	mouse which has a heterozygous *Tor1a*/*Dyt1* knock-out in one allele and *Dlx5/6-Cre*-mediated conditional knock-out in the other
***Dyt1* ChKO mice**	cholinergic cell-specific *Dyt1* conditional knock-out mice
***Dyt1* cKO mice**	cerebral cortex-specific *Dyt1* conditional knock-out mice
***Dyt1* d2KO mice**	dopamine receptor 2-expressing-cell-specific *Dyt1* conditional knock-out mice
***Dyt1* KI mice**	*Dyt1*/*Tor1a* ΔGAG heterozygous knock-in mice
***Dyt1* sKO mice**	striatum-specific *Dyt1* conditional knock-out mice
ΔGAG	in-frame trinucleotide deletion of GAG
GP	globus pallidus
GFAP	Glial Fibrillary Acidic Protein
KO mice	knock-out mice
LTD	long-term depression
7N	facial nerve nucleus
NA	not available
N-CKO mice	*Nestin-cre +/− Dyt1 loxP −*/Δ mice
PB	phosphate buffer
RN	red nucleus

WT mice	wild-type mice

References

[1]. Breakefield XO, Blood AJ, Li Y, Hallett M, Hanson PI, Standaert DG, The pathophysiological basis of dystonias, Nat Rev Neurosci 9(3) (2008) 222–34. [PubMed: 18285800]

[2]. Bressman SB, Sabatti C, Raymond D, de Leon D, Klein C, Kramer PL, Brin MF, Fahn S, Breakefield X, Ozelius LJ, Risch NJ, The DYT1 phenotype and guidelines for diagnostic testing, Neurology 54(9) (2000) 1746–52. [PubMed: 10802779]

[3]. Opal P, Tintner R, Jankovic J, Leung J, Breakefield XO, Friedman J, Ozelius L, Intrafamilial phenotypic variability of the DYT1 dystonia: from asymptomatic TOR1A gene carrier status to dystonic storm, Mov Disord 17(2) (2002) 339–45. [PubMed: 11921121]

[4]. Ozelius LJ, Hewett JW, Page CE, Bressman SB, Kramer PL, Shalish C, de Leon D, Brin MF, Raymond D, Corey DP, Fahn S, Risch NJ, Buckler AJ, Gusella JF, Breakefield XO, The early-onset torsion dystonia gene (DYT1) encodes an ATP-binding protein, Nat Genet 17(1) (1997) 40–8. [PubMed: 9288096]

[5]. Calakos N, Patel VD, Gottron M, Wang G, Tran-Viet KN, Brewington D, Beyer JL, Steffens DC, Krishnan RR, Zuchner S, Functional evidence implicating a novel TOR1A mutation in idiopathic, late-onset focal dystonia, J Med Genet 47(9) (2010) 646–50. [PubMed: 19955557]

[6]. Ritz K, Gerrits MC, Foncke EM, van Ruissen F, van der Linden C, Vergouwen MD, Bloem BR, Vandenberghe W, Crols R, Speelman JD, Baas F, Tijssen MA, Myoclonus-dystonia: clinical and genetic evaluation of a large cohort, J Neurol Neurosurg Psychiatry 80(6) (2009) 653–658. [PubMed: 19066193]

[7]. Leung JC, Klein C, Friedman J, Vieregge P, Jacobs H, Doheny D, Kamm C, DeLeon D, Pramstaller PP, Penney JB, Eisengart M, Jankovic J, Gasser T, Bressman SB, Corey DP, Kramer P, Brin MF, Ozelius LJ, Breakefield XO, Novel mutation in the TOR1A (DYT1) gene in atypical early onset dystonia and polymorphisms in dystonia and early onset parkinsonism, Neurogenetics 3(3) (2001) 133–43. [PubMed: 11523564]

[8]. Doheny D, Danisi F, Smith C, Morrison C, Velickovic M, De Leon D, Bressman SB, Leung J, Ozelius L, Klein C, Breakefield XO, Brin MF, Silverman JM, Clinical findings of a myoclonus-dystonia family with two distinct mutations, Neurology 59(8) (2002) 1244–6. [PubMed: 12391355]

[9]. Isik E, Aykut A, Atik T, Cogulu O, Ozkinay F, Biallelic TOR1A mutations cause severe arthrogryposis: A case requiring reverse phenotyping, Eur J Med Genet 18 (2018) 30331–30338.

[10]. Dang MT, Yokoi F, Cheetham CC, Lu J, Vo V, Lovinger DM, Li Y, An anticholinergic reverses motor control and corticostriatal LTD deficits in Dyt1 DeltaGAG knock-in mice, Behav Brain Res 226(2) (2012) 465–72. [PubMed: 21995941]

[11]. DeAndrade MP, Trongnetrpunya A, Yokoi F, Cheetham CC, Peng N, Wyss JM, Ding M, Li Y, Electromyographic evidence in support of a knock-in mouse model of DYT1 Dystonia, Mov Disord 31(11) (2016) 1633–1639. [PubMed: 27241685]

[12]. Dang MT, Yokoi F, McNaught KS, Jengelley TA, Jackson T, Li J, Li Y, Generation and characterization of Dyt1 DeltaGAG knock-in mouse as a model for early-onset dystonia, Exp Neurol 196(2) (2005) 452–63. [PubMed: 16242683]

[13]. Song CH, Fan X, Exeter CJ, Hess EJ, Jinnah HA, Functional analysis of dopaminergic systems in a DYT1 knock-in mouse model of dystonia, Neurobiol Dis 48(1) (2012) 66–78. [PubMed: 22659308]

[14]. Yokoi F, Dang MT, Miller CA, Marshall AG, Campbell SL, Sweatt JD, Li Y, Increased c-fos expression in the central nucleus of the amygdala and enhancement of cued fear memory in Dyt1 DeltaGAG knock-in mice, Neurosci Res 65(3) (2009) 228–35. [PubMed: 19619587]

[15]. Zhang L, Yokoi F, Jin YH, Deandrade MP, Hashimoto K, Standaert DG, Li Y, Altered Dendritic Morphology of Purkinje cells in Dyt1 DeltaGAG Knock-In and Purkinje Cell-Specific Dyt1 Conditional Knockout Mice, PLoS One 6(3) (2011) e18357. [PubMed: 21479250]

[16]. Yokoi F, Yang G, Li J, DeAndrade MP, Zhou T, Li Y, Earlier onset of motor deficits in mice with double mutations in Dyt1 and Sgce, J Biochem 148(4) (2010) 459–66. [PubMed: 20627944]

[17]. Giles LM, Chen J, Li L, Chin LS, Dystonia-associated mutations cause premature degradation of torsinA protein and cell-type-specific mislocalization to the nuclear envelope, Hum Mol Genet 17(17) (2008) 2712–22. [PubMed: 18552369]

[18]. Gordon KL, Gonzalez-Alegre P, Consequences of the DYT1 mutation on torsinA oligomerization and degradation, Neuroscience 157(3) (2008) 588–95. [PubMed: 18940237]

[19]. Yokoi F, Cheetham CC, Campbell SL, Sweatt JD, Li Y, Pre-synaptic release deficits in a DYT1 dystonia mouse model, PLoS One 8(8) (2013) e72491. [PubMed: 23967309]

[20]. Yokoi F, Chen HX, Dang MT, Cheetham CC, Campbell SL, Roper SN, Sweatt JD, Li Y, Behavioral and electrophysiological characterization of Dyt1 heterozygous knockout mice, PLoS One 10(3) (2015) e0120916. [PubMed: 25799505]

[21]. Ulug AM, Vo A, Argyelan M, Tanabe L, Schiffer WK, Dewey S, Dauer WT, Eidelberg D, Cerebellothalamocortical pathway abnormalities in torsinA DYT1 knock-in mice, Proc Natl Acad Sci U S A 108(16) (2011) 6638–43. [PubMed: 21464304]

[22]. Vo A, Sako W, Dewey SL, Eidelberg D, Ulug AM, 18FDG-microPET and MR DTI findings in Tor1a+/− heterozygous knock-out mice, Neurobiol Dis 73 (2015) 399–406. [PubMed: 25447231]

[23]. Dang MT, Yokoi F, Pence MA, Li Y, Motor deficits and hyperactivity in Dyt1 knockdown mice, Neurosci Res 56(4) (2006) 470–4. [PubMed: 17046090]

[24]. Yokoi F, Dang MT, Mitsui S, Li J, Li Y, Motor deficits and hyperactivity in cerebral cortex-specific Dyt1 conditional knockout mice, J Biochem 143(1) (2008) 39–47. [PubMed: 17956903]

[25]. Yokoi F, Dang MT, Li J, Standaert DG, Li Y, Motor deficits and decreased striatal dopamine receptor 2 binding activity in the striatum-specific Dyt1 conditional knockout mice, PLoS One 6(9) (2011) e24539. [PubMed: 21931745]

[26]. Sciamanna G, Hollis R, Ball C, Martella G, Tassone A, Marshall A, Parsons D, Li X, Yokoi F, Zhang L, Li Y, Pisani A, Standaert DG, Cholinergic dysregulation produced by selective inactivation of the dystonia-associated protein torsinA, Neurobiol Dis 47(3) (2012) 416–27. [PubMed: 22579992]

[27]. Yokoi F, Oleas J, Xing H, Liu Y, Dexter KM, Misztal C, Gerard M, Efimenko I, Lynch P, Villanueva M, Alsina R, Krishnaswamy S, Vaillancourt DE, Li Y, Decreased number of striatal cholinergic interneurons and motor deficits in dopamine receptor 2-expressing-cell-specific Dyt1 conditional knockout mice, Neurobiol Dis 134 (2020) 104638. [PubMed: 31618684]

[28]. Yokoi F, Dang MT, Li Y, Improved motor performance in Dyt1 DeltaGAG heterozygous knock-in mice by cerebellar Purkinje-cell specific Dyt1 conditional knocking-out, Behav Brain Res 230(2) (2012) 389–98. [PubMed: 22391119]

[29]. Oleas J, Yokoi F, DeAndrade MP, Pisani A, Li Y, Engineering animal models of dystonia, Mov Disord 28(7) (2013) 990–1000. [PubMed: 23893455]

[30]. Oleas J, Yokoi F, DeAndrade MP, Li Y, Rodent Models of Autosomal Dominant Primary Dystonia In: Movement Disorders: Genetics and Models (LeDoux MS, ed), pp483–505, Second ed., Academic Press Elsevier, New York, 2015.

[31]. Yokoi F, Dang MT, Li J, Li Y, Myoclonus, motor deficits, alterations in emotional responses and monoamine metabolism in epsilon-sarcoglycan deficient mice, J Biochem 140(1) (2006) 141–6. [PubMed: 16815860]

[32]. Yokoi F, Dang MT, Zhou T, Li Y, Abnormal nuclear envelopes in the striatum and motor deficits in DYT11 myoclonus-dystonia mouse models, Hum Mol Genet 21(4) (2012) 916–25. [PubMed: 22080833]

[33]. DeAndrade MP, Yokoi F, van Groen T, Lingrel JB, Li Y, Characterization of Atp1a3 mutant mice as a model of rapid-onset dystonia with parkinsonism, Behav Brain Res 216(2) (2011) 659–65. [PubMed: 20850480]

[34]. Pelosi A, Menardy F, Popa D, Girault JA, Herve D, Heterozygous Gnal Mice Are a Novel Animal Model with Which to Study Dystonia Pathophysiology, J Neurosci 37(26) (2017) 6253–6267. [PubMed: 28546310]

[35]. Goodchild RE, Kim CE, Dauer WT, Loss of the dystonia-associated protein torsinA selectively disrupts the neuronal nuclear envelope, Neuron 48(6) (2005) 923–32. [PubMed: 16364897]

[36]. Pappas SS, Darr K, Holley SM, Cepeda C, Mabrouk OS, Wong JM, LeWitt TM, Paudel R, Houlden H, Kennedy RT, Levine MS, Dauer WT, Forebrain deletion of the dystonia protein

torsinA causes dystonic-like movements and loss of striatal cholinergic neurons, Elife 4 (2015) e08352. [PubMed: 26052670]

[37]. Fremont R, Tewari A, Angueyra C, Khodakhah K, A role for cerebellum in the hereditary dystonia DYT1, Elife 6 (2017) e22775. [PubMed: 28198698]

[38]. Liang CC, Tanabe LM, Jou S, Chi F, Dauer WT, TorsinA hypofunction causes abnormal twisting movements and sensorimotor circuit neurodegeneration, J Clin Invest 124(7) (2014) 3080–92. [PubMed: 24937429]

[39]. Middeldorp J, Hol EM, GFAP in health and disease, Prog Neurobiol 93(3) (2011) 421–43. [PubMed: 21219963]

[40]. Tronche F, Kellendonk C, Kretz O, Gass P, Anlag K, Orban PC, Bock R, Klein R, Schutz G, Disruption of the glucocorticoid receptor gene in the nervous system results in reduced anxiety, Nat Genet 23(1) (1999) 99–103. [PubMed: 10471508]

[41]. Bradford MM, A rapid and sensitive method for the quantitation of microgram quantities of protein utilizing the principle of protein-dye binding, Anal Biochem 72 (1976) 248–54. [PubMed: 942051]

[42]. Yokoi F, Dang MT, Liu J, Gandre JR, Kwon K, Yuen R, Li Y, Decreased dopamine receptor 1 activity and impaired motor-skill transfer in Dyt1 DeltaGAG heterozygous knock-in mice, Behav Brain Res 279 (2015) 202–10. [PubMed: 25451552]

[43]. Casper KB, McCarthy KD, GFAP-positive progenitor cells produce neurons and oligodendrocytes throughout the CNS, Mol Cell Neurosci 31(4) (2006) 676–84. [PubMed: 16458536]

[44]. Reemst K, Noctor SC, Lucassen PJ, Hol EM, The Indispensable Roles of Microglia and Astrocytes during Brain Development, Front Hum Neurosci 10 (2016) 566. [PubMed: 27877121]

[45]. Bowyer JF, Tranter KM, Sarkar S, Hanig JP, Microglial activation and vascular responses that are associated with early thalamic neurodegeneration resulting from thiamine deficiency, Neurotoxicology 65 (2018) 98–110. [PubMed: 29427613]

[46]. Paudel R, Kiely A, Li A, Lashley T, Bandopadhyay R, Hardy J, Jinnah HA, Bhatia K, Houlden H, Holton JL, Neuropathological features of genetically confirmed DYT1 dystonia: investigating disease-specific inclusions, Acta Neuropathol Commun 2 (2014) 159. [PubMed: 25403864]

[47]. Bayraktar OA, Fuentealba LC, Alvarez-Buylla A, Rowitch DH, Astrocyte development and heterogeneity, Cold Spring Harb Perspect Biol 7(1) (2014) a020362. [PubMed: 25414368]

[48]. Chaboub LS, Deneen B, Astrocyte form and function in the developing central nervous system, Semin Pediatr Neurol 20(4) (2013) 230–5. [PubMed: 24365570]

[49]. Ben Haim L, Rowitch DH, Functional diversity of astrocytes in neural circuit regulation, Nat Rev Neurosci 18(1) (2017) 31–41. [PubMed: 27904142]

[50]. Molofsky AV, Krencik R, Ullian EM, Tsai HH, Deneen B, Richardson WD, Barres BA, Rowitch DH, Astrocytes and disease: a neurodevelopmental perspective, Genes Dev 26(9) (2012) 891–907. [PubMed: 22549954]

[51]. Verkhratsky A, Nedergaard M, Physiology of Astroglia, Physiol Rev 98(1) (2018) 239–389. [PubMed: 29351512]

[52]. Valentino KL, Jones EG, Kane SA, Expression of GFAP immunoreactivity during development of long fiber tracts in the rat CNS, Brain Res 285(3) (1983) 317–36. [PubMed: 6627026]

[53]. Sofroniew MV, Vinters HV, Astrocytes: biology and pathology, Acta Neuropathol 119(1) (2010) 7–35. [PubMed: 20012068]

[54]. Osborn LM, Kamphuis W, Wadman WJ, Hol EM, Astrogliosis: An integral player in the pathogenesis of Alzheimer's disease, Prog Neurobiol 144 (2016) 121–41. [PubMed: 26797041]

[55]. Feoli AM, Leite MC, Tramontina AC, Tramontina F, Posser T, Rodrigues L, Swarowsky A, Quincozes-Santos A, Leal RB, Gottfried C, Perry ML, Goncalves CA, Developmental changes in content of glial marker proteins in rats exposed to protein malnutrition, Brain Res 1187 (2008) 33–41. [PubMed: 18021757]

[56]. Ranade SC, Sarfaraz Nawaz M, Kumar Rambtla P, Rose AJ, Gressens P, Mani S, Early protein malnutrition disrupts cerebellar development and impairs motor coordination, Br J Nutr 107(8) (2012) 1167–75. [PubMed: 22050885]

[57]. Mendonca JE, Vilela MC, Bittencourt H, Lapa RM, Oliveira FG, Alessio ML, Guedes RC, De Oliveira Costa MS, Da Costa BL, GFAP expression in astrocytes of suprachiasmatic nucleus and medial preoptic area are differentially affected by malnutrition during rat brain development, Nutr Neurosci 7(4) (2004) 223–34. [PubMed: 15682649]

HIGHLIGHTS

- Culling during the lactation improved the survival of the underweight N-CKO mice.
- Surviving adult N-CKO mice did not show overt “dystonic” symptoms.
- N-CKO mice with culling showed normal distributions of astrocytes & apoptotic cells.
- Neurodegeneration likely is not involved in the pathogenesis of DYT1 dystonia.
- N-CKO mouse is not an appropriate model of DYT1 dystonia.

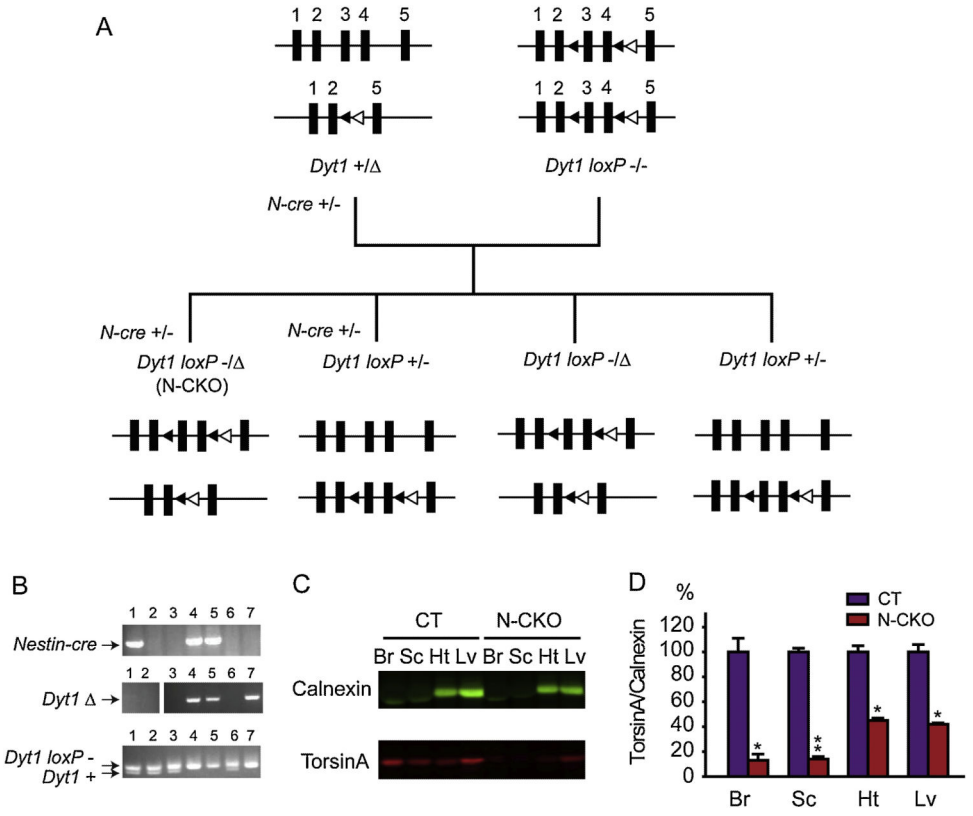

Figure 1.

(**A**) Breeding scheme to generate N-CKO mice. *Nestin-cre* (*N-cre*) +/− *Dyt1* +/Δ male mice were crossed with *Dyt1 loxP* −/− female mice to generate *N-cre* +/− *Dyt1 loxP* −/Δ (N-CKO), *N-cre* +/− *Dyt1 loxP* +/−, *Dyt1 loxP* −/Δ, and *Dyt1 loxP* +/− mice. Notations; *Dyt1* + and *Dyt1 loxP* +: wild-type of *Dyt1* (*Tor1a*) allele; *Dyt1 loxP* -: floxed *Dyt1* allele, before conditionally knocked-out; *Dyt1* Δ: constitutive knock-out of *Dyt1* allele (instead of ΔGAG). (**B**) PCR-based tail DNA genotyping of *Nestin-cre*, *Dyt1* Δ, *Dyt1 loxP* - and *Dyt1* + loci. Lane 1: *Nestin-cre* +/− *Dyt1 loxP* +/−; lanes 2, 3, 6: *Dyt1 loxP* +/−; lanes 4, 5: *Nestin-cre* +/− *Dyt1 loxP* −/Δ (N-CKO); lane 7: *Dyt1 loxP* −/Δ. (**C**) Western blot analysis of torsinA and calnexin in the brain (Br), spinal cord (Sc), heart (Ht) and liver (Lv) from CT (*Dyt1 loxP* +/−) and N-CKO mice at P0. (**D**) Quantification of the western blot data. The torsinA level in each sample was standardized with calnexin level and normalized to that in CT mice. Means ± standard errors are shown. *$p < 0.05$, **$p < 0.01$.

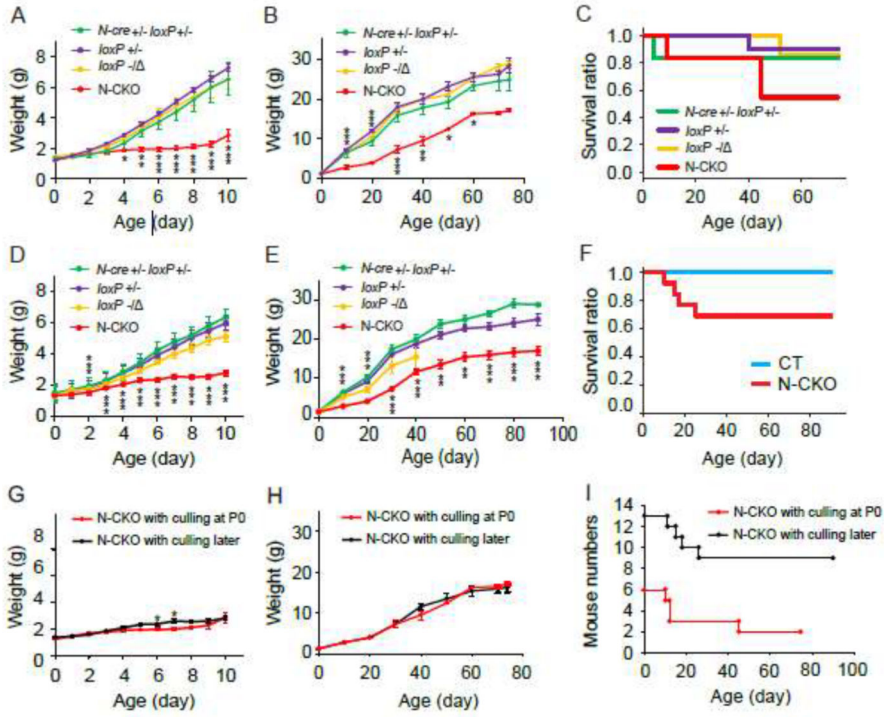

Figure 2.

(**A-C**). N-CKO and CT littermate mice with culling at P0. (**A**) Neonatal growth curve. Body weight of each genotype mice was plotted. (**B**) Growth curve for 74 days. (**C**) Survival ratio of the first batch shown in A and B. (**D-F**). Mice culled after P9. (**D**) Neonatal growth curve. Body weight of each genotype was plotted. (**E**) Growth curve for 90 days. (**F**) Survival ratio of the second batch. CT mice contain three control genotypes, *i.e. N-cre* +/− *Dyt1 loxP* +/−, *Dyt1 loxP* +/−, and *Dyt1 loxP* −/Δ mice, shown in D and E. (**G-I**) Comparison of N-CKO mice between the first batch with culling at P0 (red) and the second batch with culling later (after P9; black). (**G**) Comparison of the neonatal growth curves between the first batch (red) and the second batch (black). (**H**) Comparison of the growth curves between the first batch (red) and the second batch (black) for 74 days. (**I**) The numbers of N-CKO mice in the first batch (red) and the second batch (black). Means ± standard errors are shown in A, B, D, E, G, H. *$p < 0.05$, **$p < 0.01$, ***$p < 0.001$.

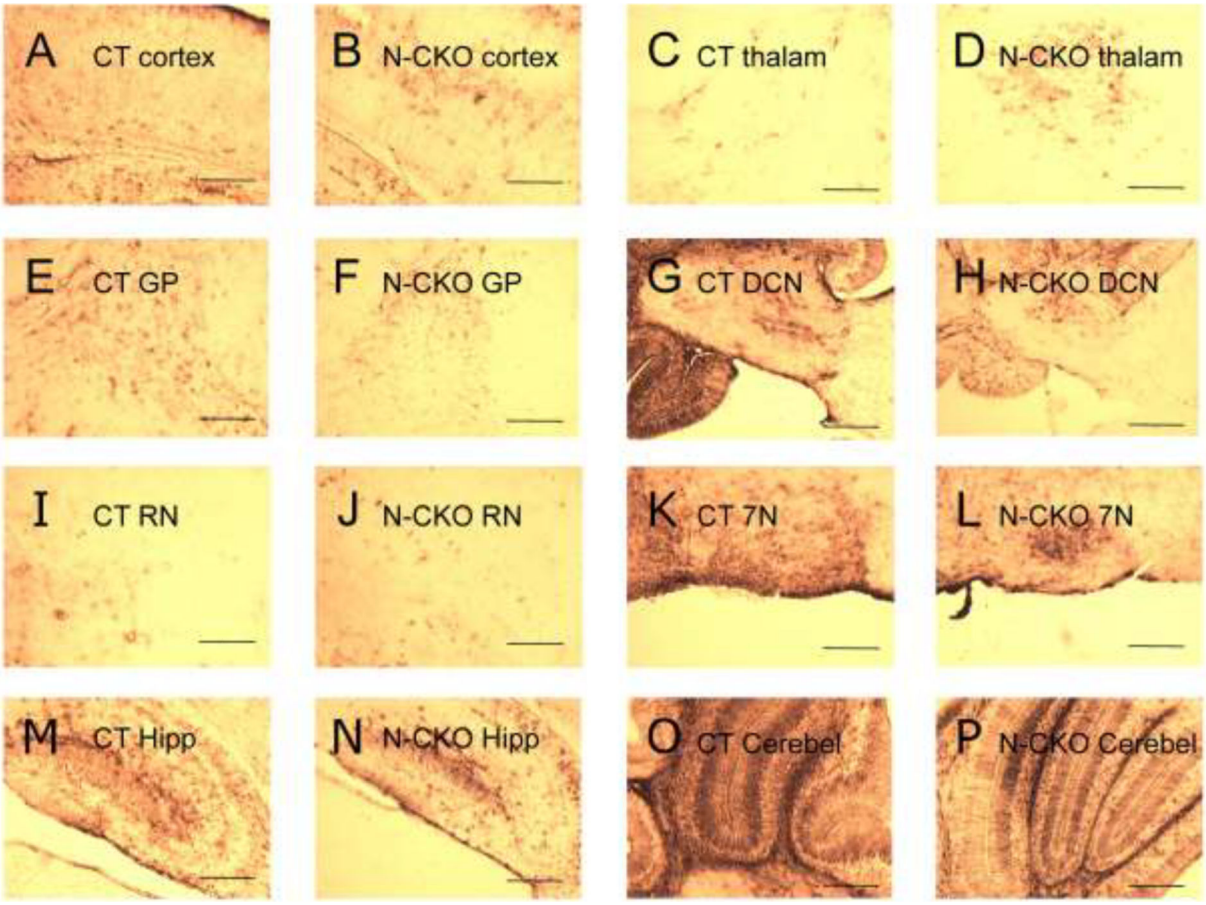

Figure 3.

Representative images of the GFAP-positive cells in CT and N-CKO mice with culling. (**A**) CT, the cerebral cortex. (**B**) N-CKO, the cerebral cortex. (**C**) CT, thalamus. (**D**) N-CKO, thalamus. (**E**) CT, globus pallidus (GP). (**F**) N-CKO, GP. (**G**) CT, deep cerebellar nuclei (DCN). (**H**) N-CKO, DCN. (**I**) CT, red nucleus (RN). (**J**) N-CKO, RN. (**K**) CT, facial nerve nucleus (7N). (**L**) N-CKO, 7N. (**M**) CT, hippocampus. (**N**) N-CKO, the hippocampus. (**O**) CT, cerebellum. (**P**) N-CKO, cerebellum. WT mouse is shown as a representative CT. The images were taken with 10× objective lens. The scale bars indicate 250 μm.

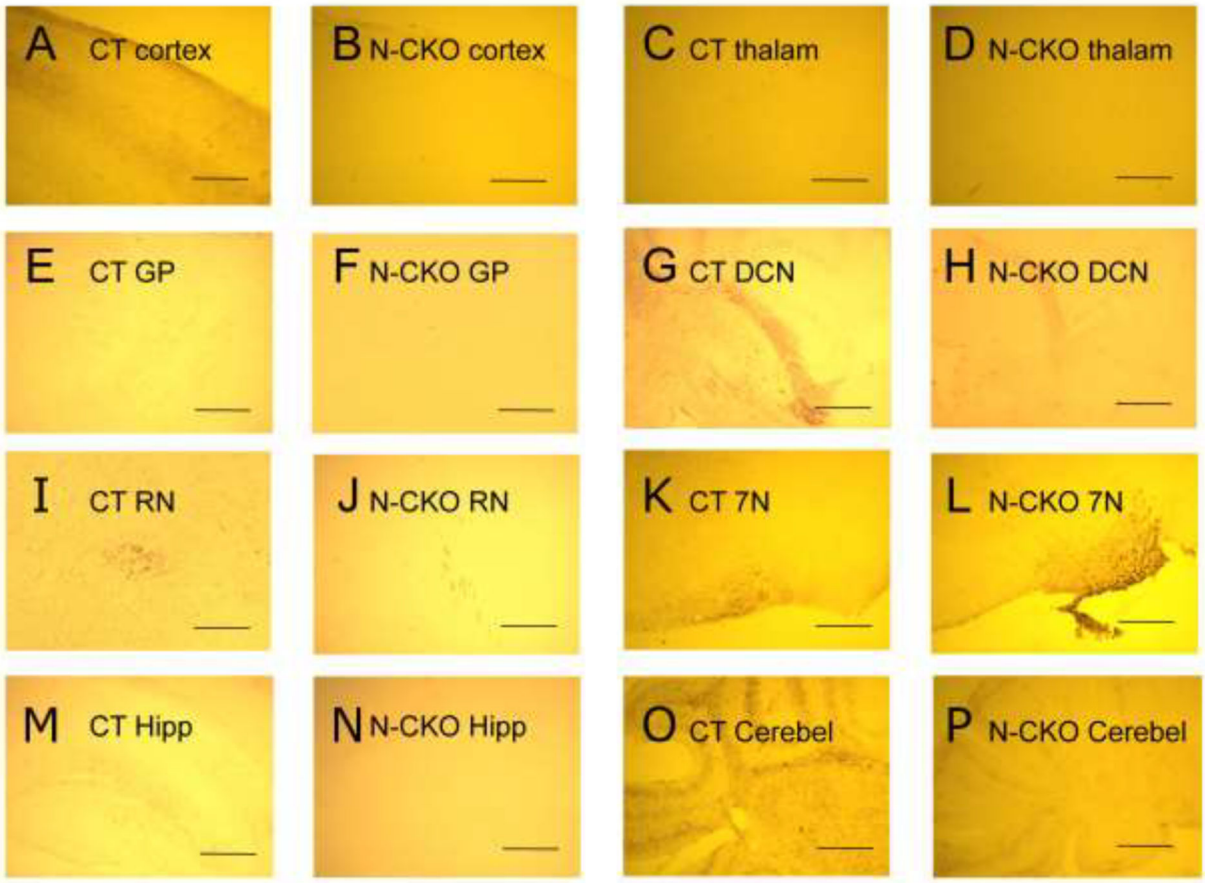

Figure 4.

Representative images of the CC3-positive cells in CT and N-CKO mice with culling. (**A**) CT, the cerebral cortex. (**B**) N-CKO, the cerebral cortex. (**C**) CT, thalamus. (**D**) N-CKO, thalamus. (**E**) CT, globus pallidus (GP). (**F**) N-CKO, GP. (**G**) CT, deep cerebellar nuclei (DCN). (**H**) N-CKO, DCN. (**I**) CT, red nucleus (RN). (**J**) N-CKO, RN. (**K**) CT, facial nerve nucleus (7N). (**L**) N-CKO, 7N. (**M**) CT, hippocampus. (**N**) N-CKO, hippocampus. (**O**) CT, cerebellum. (**P**) N-CKO, cerebellum. WT mouse is shown as a representative CT. The images were taken with 10× objective lens. The scale bars indicate 250 μm.

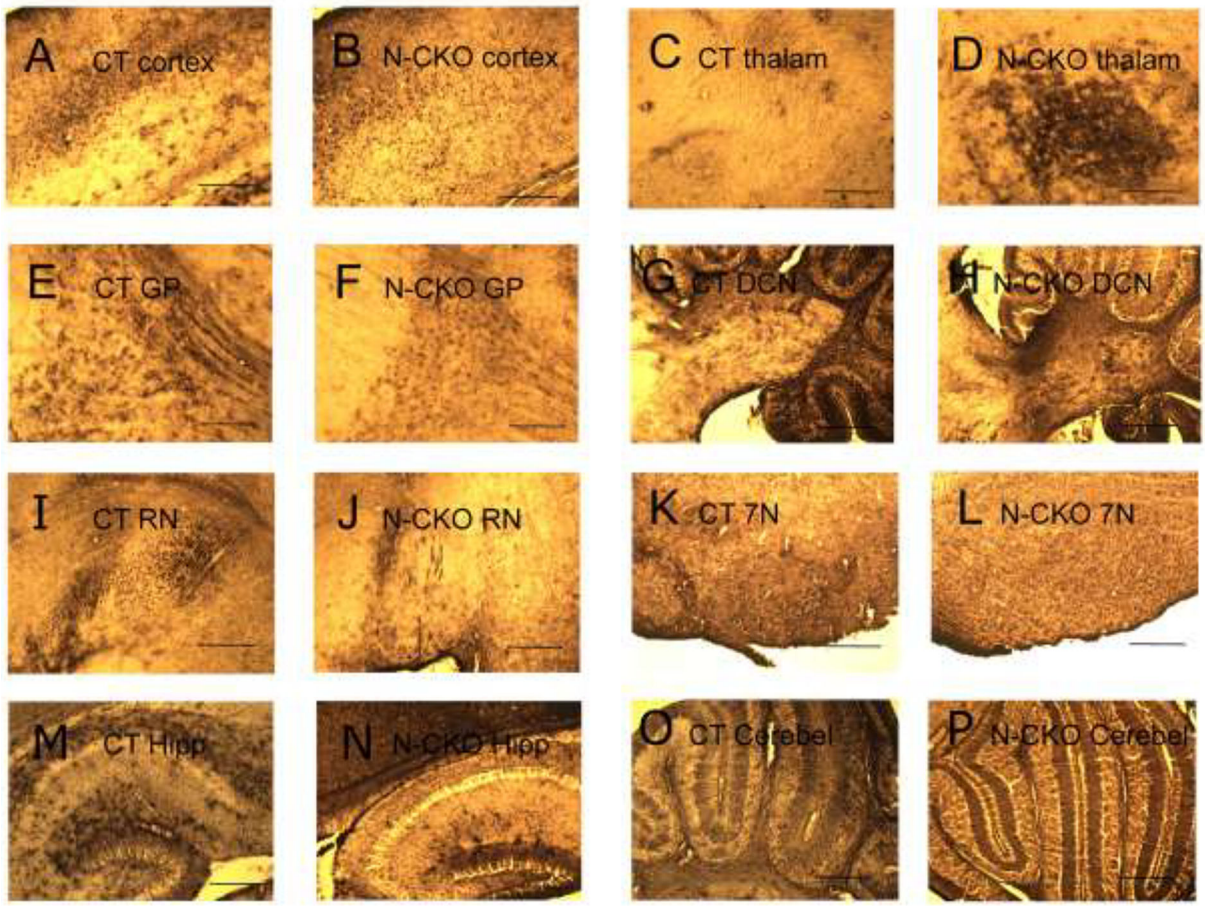

Figure 5.

Representative images of the GFAP-positive cells in CT and N-CKO mice without culling. (**A**) CT, the cerebral cortex. (**B**) N-CKO, the cerebral cortex. (**C**) CT, thalamus. (**D**) N-CKO, thalamus. (**E**) CT, globus pallidus (GP). (**F**) N-CKO, GP. (**G**) CT, deep cerebellar nuclei (DCN). (**H**) N-CKO, DCN. (**I**) CT, red nucleus (RN). (**J**) N-CKO, RN. (**K**) CT, facial nerve nucleus (7N). (**L**) N-CKO, 7N. (**M**) CT, hippocampus. (**N**) N-CKO, the hippocampus. (**O**) CT, cerebellum. (**P**) N-CKO, cerebellum. *Dyt1 loxP*+/− mouse is shown as a representative CT. The images were taken with 10× objective lens. The scale bars indicate 250 μm.

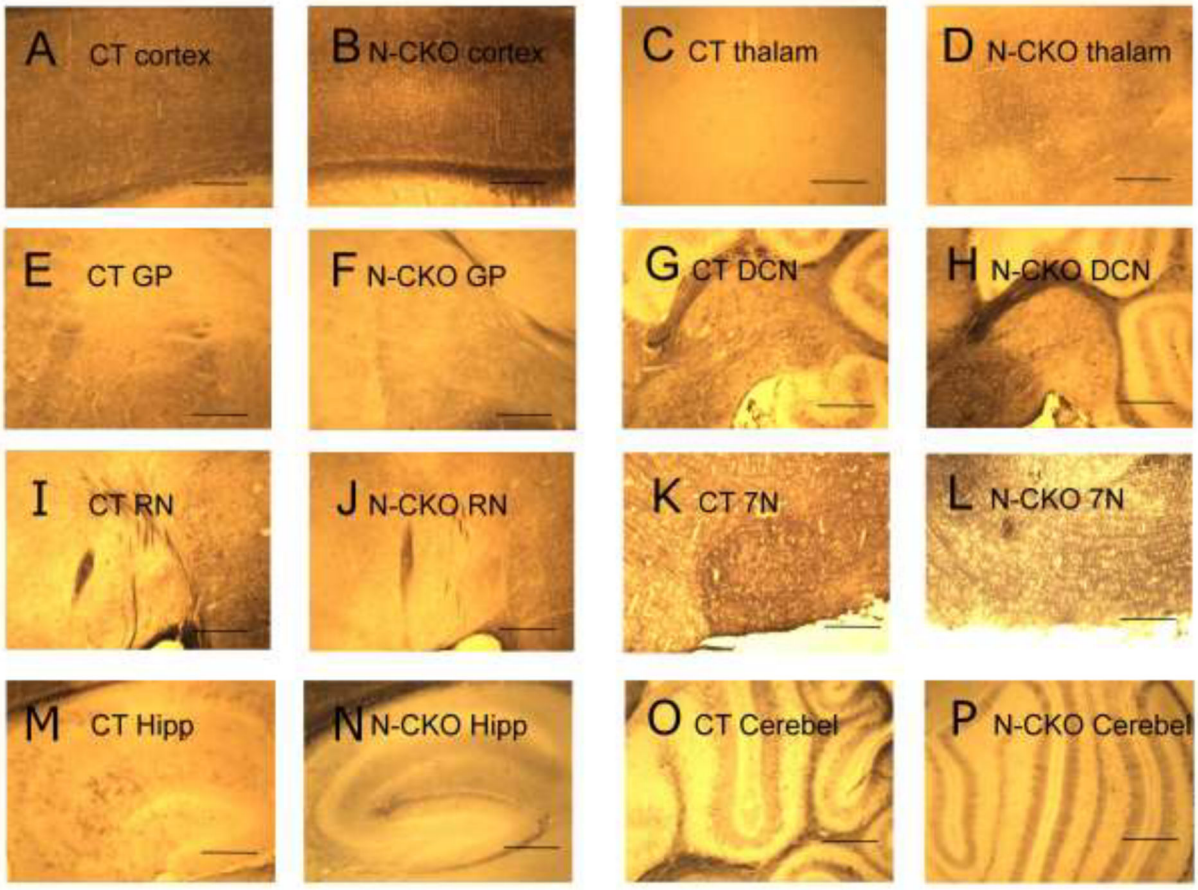

Figure 6.

Representative images of the CC3-positive cells in CT and N-CKO mice without culling. (**A**) CT, the cerebral cortex. (**B**) N-CKO, the cerebral cortex. (**C**) CT, thalamus. (**D**) N-CKO, thalamus. (**E**) CT, globus pallidus (GP). (**F**) N-CKO, GP. (**G**) CT, deep cerebellar nuclei (DCN). (**H**) N-CKO, DCN. (**I**) CT, red nucleus (RN). (**J**) N-CKO, RN. (**K**) CT, facial nerve nucleus (7N). (**L**) N-CKO, 7N. (**M**) CT, hippocampus. (**N**) N-CKO, hippocampus. (**O**) CT, cerebellum. (**P**) N-CKO, cerebellum. *Dyt1 loxP*+/− mouse is shown as a representative CT. The images were taken with 10× objective lens. The scale bars indicate 250 μm.